Anticancer roles of let-7f-1-3p in non-small cell lung cancer via direct targeting of integrin β1

YANAN YANG[1*], YUANRONG LIU[1*], NING XIE[2*], LIYING SHAO[1], HANG SUN[1], YUBO WEI[1], YUNXIAO SUN[3], PINGYU WANG[1], YUNFEI YAN[1], SHUYANG XIE[1] and YOUJIE LI[1]

[1]Key Laboratory of Tumor Molecular Biology, Department of Biochemistry and Molecular Biology, Binzhou Medical University, Yantai, Shandong 264003; [2]Department of Thoracic Surgery, Yantaishan Hospital, Yantai, Shandong 264001; [3]Department of Pediatrics, Yantai Affiliated Hospital of Binzhou Medical University, Yantai, Shandong 264100, P.R. China

Received April 28, 2020; Accepted June 4, 2021

DOI: 10.3892/etm.2021.10740

Abstract. Lung cancer is one of the most common types of cancer, with the highest mortality rate worldwide. MicroRNAs play notable roles in the chemotherapeutic effects of anticancer drugs. The present study used reverse transcription-quantitative PCR, western blotting and cell migration and invasion assays to reveal the role of let-7f-1-3p in non-small cell lung cancer (NSCLC) and explore the effect of let-7f-1-3p on doxorubicin (DOX) treatment. It was demonstrated that the levels of let-7f-1-3p in carcinoma tissues were lower compared with those in paracarcinoma tissues. Thus, let-7f-1-3p may act as a suppressor gene. The present study also explored the role of let-7f-1-3p in A549 and NCI-H1975 cells. Results revealed that let-7f-1-3p could inhibit the viability, migration and invasion of NSCLC cells and induce their apoptosis. Integrin β1 acted as a target gene regulated by let-7f-1-3p. This suggested that let-7f-1-3p could enhance DOX-inhibited cell viability, migration and invasion *in vitro*. Overall, the present study demonstrated that let-7f-1-3p may act as a target for drug design and lung cancer therapy.

Correspondence to: Dr Shuyang Xie or Dr Youjie Li, Key Laboratory of Tumor Molecular Biology, Department of Biochemistry and Molecular Biology, Binzhou Medical University, 346 Guanhai Road, Laishan, Yantai, Shandong 264003, P.R. China
E-mail: shuyangxie@aliyun.com
E-mail: youjie1979@163.com

*Contributed equally

Abbreviations: miRNAs, microRNAs; NSCLC, non-small cell lung cancer; DOX, doxorubicin; ITGB1, integrin β1; RT-qPCR, reverse transcription-quantitative polymerase chain reaction; HBE, human bronchial epithelial

Key words: let-7f-1-3p, DOX, ITGB1, NSCLC, chemotherapy

Introduction

Lung cancer is the leading cause of cancer-associated mortality, accounting for 18.4% of total cancer deaths according to a 2018 Global Cancer Statistics report on the global burden of cancer (1). Non-small cell lung cancer (NSCLC) accounts for ~85% of all lung cancer cases (2,3). Aside from surgical resection, which is the gold standard for NSCLC treatment, chemoradiotherapy, EGFR-tyrosine kinase inhibitors and anaplastic lymphoma kinase inhibitors are common NSCLC treatment strategies (4). However, the prognosis of patients with NSCLC remains poor. Therefore, the molecular mechanisms of NSCLC should be investigated to develop new treatment and therapeutic targets for NSCLC.

MicroRNAs (miRNAs/miRs) are endogenous small non-coding RNAs with a length of 20-24 nucleotides that play important roles in numerous biological processes (2). The regulatory roles of miRNAs involve the negative regulation of gene expression by binding to the 3' untranslated region (UTR) of target mRNAs (5). miRNAs may be key mediators of tumor development in various types of cancer, such as NSCLC (6,7), prostate cancer (8), colorectal cancer (9) and ovarian cancer (10). According to the miRbase database, the let-7f-1 family includes two types, namely, let-7f-5p and let-7f-1-3p. Let-7f-5p is involved in regulating all types of biological disease processes (11-18), including cancer (17,18). Moreover, according to the tumor suppressor gene, tumor-associated gene and TRANSFAC databases, let-7f-1-3p is downregulated in colorectal cancer tissues (19). However, the involvement of let-7f-1-3p in NSCLC development is poorly understood. Thus, the function and potential application of let-7f-1-3p in NSCLC biology should be extensively investigated.

Integrin β1 (ITGB1) is considered a potential oncoprotein that promotes the malignant progression of cancer (20), particularly in cancer cell invasion and migration (21). ITGB1 is activated during the tumorigenesis and migration of gastric cancer via lumican (22). The more ITGB1 is aggregated by C-X-C motif chemokine 12, the more invasion is promoted (23). In addition, ITGB1 is stabilized to promote small-cell lung cancer migration by cullin-5 (21), and cellular retinoic acid binding protein 1 requires Hu antigen R to promote the ITGB1 expression necessary for lung cancer metastasis (24).

The present study described the role of let-7f-1-3p in suppressing the cancer progression of NSCLC by regulating ITGB1. Moreover, let-7f-1-3p-overexpression combined with doxorubicin (DOX)-induced apoptosis of A549 cells provided new insights into the mechanism of miRNA-mediated tumor suppression and a new target for NSCLC treatment .

Materials and methods

Patients and tissue samples. Tumorous lung tissue and matched paratumor tissues (5 cm away from the tumor tissue) were collected from 15 patients (8 female and 7 male) who underwent curative surgery for NSCLC at Yantaishan Hospital, The Teaching Hospital of Binzhou Medical University (Yantai, China). None of the patients were subjected to radiotherapy and chemotherapy before the operation. Informed consent was obtained from all the participants before the study. The samples were collected from May to August in 2019. This study was approved by The Ethics Committee of Binzhou Medical University (Yantai, China; approval number: 2018-07-06). The clinicopathological data of the patients is presented in Table I. The data was assessed by a pathologist at Yantaishan Hospital (Yantai, China).

Cell culture. The NSCLC cell line A549 and 293T cells were obtained from the Shanghai Institute of Biochemistry and Cell Biology. NCI-H1975 was purchased from Procell Life Science & Technology Co., Ltd. Human bronchial epithelial (HBE)135-E6E7 cells were obtained from the American Type Culture Collection (cat. no. ATCC® CRL-2741™). The NSCLC cells were maintained in RPMI-1640 medium (Gibco; Thermo Fisher Scientific Inc.) supplemented with 10% fetal bovine serum (Gibco; Thermo Fisher Scientific Inc.) and anti-mycoplasma reagent (cat. no. HB-SV1000; Hanbio Biotechnology Co., Ltd.). All the cells were maintained in a humidified incubator at 37˚C under 5% CO_2 condition. let-7f-1-3p mimics, let-7f-1-3p inhibitors and negative controls (NC) were synthesized by Shanghai GenePharma Co., Ltd. The corresponding sequences were as follows: let-7f-1-3p mimic, sense, 5'-CUA UACAAUCUAUUGCCUUCCC-3', and antisense, 5'-GAA GGCAAUAGAUUGUAUAGUU; let-7f-3p inhibitor, 5'-GGG AAGGCAAUAGAUUGUAUAG-3'; mimic NC (miRNA mimic negative control), sense, 5'-UUCUUCGAACGUGUC ACGUTT-3', and antisense, 5'-ACGUGACACGUUCGGAGA ATT-3'; inhibitor NC (scrambled), CAGUACUUUUGUGUA GUACAA. The final concentration of transfected miRNA mimics/inhibitors was 30 nM. pcDNA3.1-ITGB1-3*Flag and negative controls (pcDNA3.1-3*Flag) were purchased by Shanghai GeneChem Co., Ltd. Plasmid (2 μg) was used for transfection. Transfection was performed in triplicate at ~60% confluence using Lipofectamine® 2000 (Invitrogen; Thermo Fisher Scientific, Inc.) in accordance with the manufacturer's protocol. The transfection mixture was added dropwise to the experimental wells and mixed and incubated at 37˚C, 5% CO_2 for 6-10 h. The transfection solution was aspirated and 2 ml of RPMI-1640 culture solution containing 10% fetal bovine serum was added to the wells and incubated at 37˚C, 5% CO_2 for 24-48 h. The cells were observed under a light microscope (BX43; Olympus, Inc.) (magnification, x100). Following this the cells were used for subsequent experimentation.

Reverse transcription-quantitative (RT-q)PCR. NSCLC cells were incubated at 37˚C 5% CO_2 with let-7f-1-3p mimics or let-7f-1-3p inhibitor and used in subsequent experiments after 48 h of transfection. Small RNA was purified using RNAiso for small RNA reagent (Takara Biotechnology Co., Ltd.). The primers used to amplify let-7f-1-3p (Shanghai GenePharma Co., Ltd.) were as follows: Forward, 5'-CTATACAATCTA TTGCCTTCCC-3', and reverse, 5'-AACATGTACAGTCCA TGGATG-3'. Human 5S ribosomal (r)RNA served as the positive control. The primers used to amplify 5S rRNA (Shanghai GenePharma Co., Ltd.) were as follows: Forward, 5'-GCC ATACCACCCTGAACG-3', and reverse, 5'-AACATGTAC AGTCCATGGATG-3'. According to the Poly(A) Polymerase (cloned) 2 U/ul kit manual (cat. no. AM2030; Invirtogen; Thermo Fisher Scientific Inc.), a poly A tail was added to the 3' end of the miRNA. The subsequent reverse transcription (PrimeScript™ RT reagent Kit with gDNA Eraser, cat. no. RR047A; Takara Biotechnology Inc.) was the same as the reverse transcription of total RNA and was performed according to the manufacturer's protocol. Total RNA was purified using TRIzol® reagent (Takara Biotechnology Co., Ltd.). The primers used to magnify ITGB1 (Shanghai GenePharma Co., Ltd.) were as follows: Forward, 5'-AAA ATGTAACCAACCGTAGCAAAG-3', and reverse, 5'-GAC AGGTCCATAAGGTAGTAGA-3'. Human GAPDH mRNA served as the positive control. The primers used to amplify GAPDH mRNA (Shanghai GenePharma Co., Ltd.) were as follows: Forward, 5'-GTCTTCACCACCATGGAGAAGG-3', and reverse, 5'-GCCTGCTTCACCACCTTCTTGA-3. TB Green (cat. no. RR420A; Takara Bio Inc.) was used for the RT-qPCR reaction. qPCR was performed on a StepOnePlus Real-Time PCR System (Thermo Fisher Scientific, Inc.) under the following reaction conditions: Initial denaturation at 95˚C for 10 min, followed by 40 cycles of 95˚C for 15 sec and fluorescence signal acquisition at 60˚C for 1 min. The relative expression levels of the gene of interest were calculated using the $2^{-\Delta\Delta Ct}$ method (2).

MTT assay. A549 and NCI-H1975 cells were seeded onto 96-well plates at 4,000 cells/well at 24 h after transfection. MTT assay was used to confirm cell viability at 48 h after the cells were plated. Purple formazan was dissolved with dimethyl sulfoxide (DMSO; Sigma-Aldrich; Merck KGaA). The absorbance at 491 nm was measured using a Multiskan FC microplate reader (Thermo Fisher Scientific, Inc.).

Colony formation assay. For the colony formation assay, the A549 and NCI-H1975 cells were plated onto a 10-cm cell culture dish at a density of 1,500 cells/plate at 24 h after transfection. The RPMI-1640 culture solution containing 10% fetal bovine serum was replaced every 4 days. After ~12 days, the majority of the cell clones contained >40 cells. The plate was gently washed with 1X PBS and 4% paraformaldehyde was used to fix the clones for 1 h at room temperature, which were subsequently stained with crystal violet for ~30 min at room temperature. Images were captured and the clones were quantified by eye.

Western blotting. A549 and NCI-H1975 cells were lysed using RIPA lysis buffer (Beijing Solarbio Science & Technology

Table I. Clinicopathological data of patients with non-small cell lung cancer.

Sample no.	Sex	Age, years	Tumor stage	TNM stage	Tumor grade
1	Female	62	IIA	T2aN1M0	G1
2	Female	50	IB	T2aN0M0	G1
3	Female	57	IA	T1aN0M0	G1
4	Female	56	IB	T2aN0M0	G1
5	Female	65	IIA	T2aN1M0	G1
6	Female	67	IA	T1aN0M0	G1
7	Female	57	IA	T1aN0M0	G1
8	Female	76	IB	T2aN0M0	G1
9	Male	61	IA	T1aN0M0	G1
10	Male	39	IA	T2aN0M0	G1
11	Male	64	IA	T1aN0M0	G1
12	Male	62	IA	T1aN0M0	G1
13	Male	66	IA	T1aN0M0	G1
14	Male	61	IB	T2aN0M0	G1
15	Male	64	IIA	T1bN0M0	G1

TNM, tumor-node-metastasis.

Co., Ltd.) with a complete protease inhibitor cocktail tablet (cat. no. CORO; MilliporeSigma) on ice. BCA protein concentration determination kit (cat. no. P0012; Beyotime Institute of Biotechnology) to detect protein concentration. The absorbance at 560 nm was measured using a Multiskan FC microplate reader (Thermo Fisher Scientific, Inc.). Total protein (50 μg/lane) was separated on a 10% SDS-PAGE gel, transferred to a PVDF membrane and blocked with 5% skim milk powder blocking solution for 2-3 h at room temperature. The primary antibodies were incubated with the membrane at 4˚C overnight. Rabbit antibodies against GAPDH (1:5,000; cat. no. AP0063), ITGB1 (1:2,000; cat. no. BS9835M), MYC (1:800; cat. no. BS2462), Bax (1:800; cat. no. BS2538; all Bioworld Technology, Inc.), BCL2 (1:2,000; cat. no. 12789-1-AP; ProteinTech Group, Inc.), E-cadherin and vimentin (both 1:1,000; cat. no. 9782; Cell Signaling Technology, Inc.) were used. The membranes were then incubated with goat anti-rabbit HRP-conjugated secondary antibody (1:2,000; cat. no. SA00001-2; ProteinTech Group, Inc.) for 2 h at 4˚C. GAPDH was used as an internal reference. The chemiluminescence substrate a Chemistar™ High-sig ECL Western Blotting substrate (cat. no. 180-5001; Tanon Science and Technology Co., Ltd.) with the Tanon 4600 series automatic chemiluminescence/fluorescence image analysis system (Tanon Science and Technology Co., Ltd.) was used for detection and analysis.

Cell migration and invasion assays. The cells were transfected with oligonucleotides and treated with DOX (200 ng/ml) for 36 h. Subsequently, 50,000 cells were resuspended in a serum-free medium and plated in the upper chamber of a modified two-compartment Corning Transwell plate (24-well; cat. no. 3428; Corning, Inc.) with a pore size of 8.0 μm. The lower chamber medium contained 20% fetal bovine serum (Gibco; Thermo Fisher Scientific Inc.). For the invasion experiment, Matrigel was diluted with RPMI-1640 at a ratio of 1:3 on ice and pre-coated onto the chamber on the Transwell plate at 37˚C, 5% CO_2 for 2 h for subsequent experiments. Unlike the invasion experiment, the migration experiment did not require Matrigel. After incubation at 37˚C 5% CO_2 for 24 h, the migration test setup was removed from the culture plate, and the invasion test setup was removed after 48 h of incubation at 37˚C and 5% CO_2. The cells that were transferred to the lower chamber were washed with 1X PBS, fixed in 4% paraformaldehyde for 30 min at room temperature and stained with crystal violet for 30 min at room temperature. The cells were rinsed gently with ultrapure water and dried and a fully automatic upright fluorescent microscope (DM6000 B; Leica Microsystems Inc.) (magnification, x20) was used with randomly switching 5 fields of views to take images that were then visually counted.

Luciferase reporter assay. 293T cells were cultured in a 10-cm culture dish to 90% confluence, trypsin (cat. no. 25200056; Gibco; Thermo Fisher Scientific Inc.) digested for 30 sec and counted with a beef abalone counter. A total of ~5x10^4 cells were added to each well of a six-well plate, and transfection was performed after 16 h of culture at 37˚C and 5% CO_2. let-7f-1-3p (sense, 5'-CUAUACAAUCUAUUGCCUUCCC-3' and antisense, 5'-GAAGGCAAUAGAUUGUAUAGUU) or NC (sense, 5'-UUCUUCGAACGUGUCACGUTT-3' and antisense, 5'-ACGUGACACGUUCGGAGAATT-3') were co-transfected with GP-miRGLO-ITGB1 wild-type (WT) or GP-miRGLO-ITGB1 mutant (MUT) (Shanghai GeneChem Co., Ltd.). Plasmid (2 μg), miRNA mimic/NC (30 nM) were transfected using Lipofectamine® 2000 (Invitrogen; Thermo Fisher Scientific Inc.) and replaced with a whole medium after 8 h, further cultured for 36 h, lysed and collected using a Dual-Luciferase® Reporter Assay System (cat. no. E1910; Promega Corporation) in accordance with the manufacturer's instructions. *Renilla luciferase* activity was used for normalization.

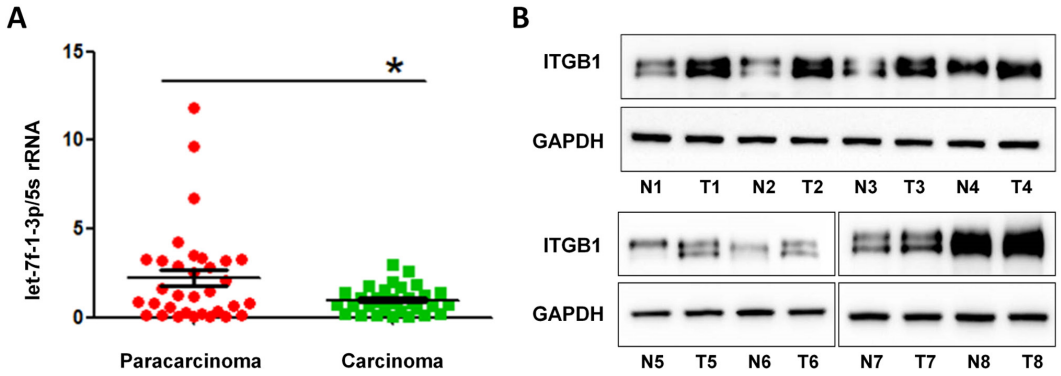

Figure 1. let-7f-1-3p is significantly downregulated and ITGB1 is upregulated in lung adenocarcinoma tissues. (A) let-7f-1-3p expression profiles in lung adenocarcinoma tissues (n=15) and normal adjacent control tissues (n=15) were detected using reverse transcription-quantitative PCR. (B) Expression levels of ITGB1 protein in lung adenocarcinoma were higher in lung adenocarcinoma tissues (n=8) than in paracancerous tissues. *P<0.05. NSCLC, non-small cell lung cancer; N, NSCLC adjacent tissues; T, NSCLC tissues; ITGB1, integrin β1; rRNA, ribosomal RNA.

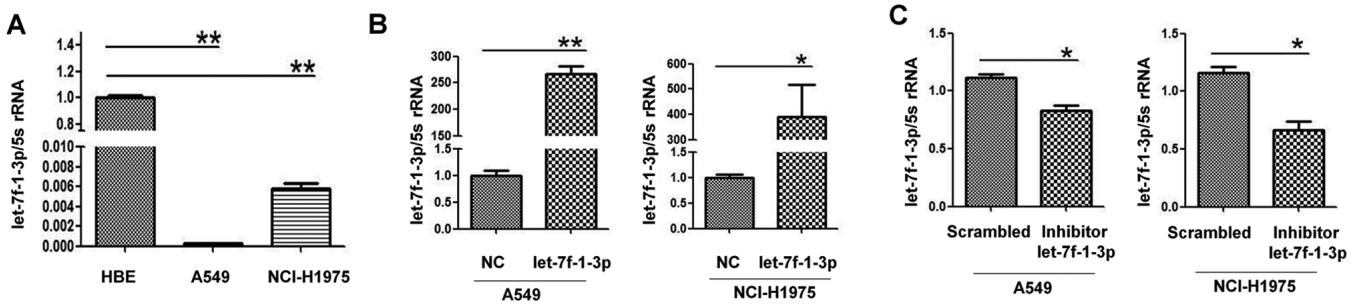

Figure 2. Expression levels of let-7f-1-3p decrease in NSCLC cell lines. (A) RT-qPCR results of let-7f-1-3p in HBE, A549 and NCI-H1975 cells. (B) RT-qPCR analysis of exogenous let-7f-1-3p expression after transfection with let-7f-1-3p mimics and NC in A549 and NCI-H1975 cells. (C) let-7f-1-3p expression levels were detected after let-7f-1-3p transfection with the let-7f-1-3p inhibitor and scrambled NC in A549 and NCI-H1975 cells. *P<0.05, **P<0.01. NSCLC, non-small cell lung cancer; RT-qPCR, reverse transcription-quantitative PCR; NC, negative control; HBE, human bronchial epithelial; rRNA, ribosomal RNA.

Tumor experiment involving nude mice. A total of 12 SPF BALB/c nude mice with an average weight of 14 g (6 weeks old; male) were purchased from GemPharmatech Co., Ltd. (animal certificate no. 201904776). Mice were raised in SPF conditions with a 12/12 h light/dark cycle and randomly divided into cages, given SPF immunodeficiency mouse feed (Beijing Keao Xieli Feed Co., Ltd.) and the drinking water was autoclaved. All animal experiments in the present study were approved by The Committee on the Ethics of Animal Experiments of Binzhou Medical University. Mice were randomly divided into 2 groups, NC injection group and let-7f-1-3p injection group, with 6 animals in each group. A549 cells that were transiently transfected with let-7f-1-3p or NC were thoroughly digested and counted through trypsinization. The cell concentration was adjusted to $5x10^7$/ml in 1X PBS, and 100 μl of cells was injected into the shoulder of each mouse. Nude mice were anesthetized via intraperitoneal injection of 1% sodium pentobarbital (50 mg/kg) for ~10 min. A Vernier caliper was used to measure tumor width, and tumor volume was calculated using the following formula: Tumor volume=(length x width^2)/2. After 9 weeks, the mouse tumor had grown to ~40 mm^3. The transfection solution prepared by let-7f-1-3p mimics or NC and Lipofectamine 2000 was diluted to 100 μl with PBS to make the final concentration of mimics 1.0 μM, and then injected at multiple sites of the tumor twice a week (25). At the same time, the mice in the NC injection group/let-7f-1-3p injection group were randomly divided into a DOX-administered group or a saline-administered group with 3 mice in each group and treated intraperitoneally at a dose of 1.5 mg/kg body weight. The control group was given the same volume of physiological saline every 3 days. The treatments were continuously administered for 2 weeks, and every 3 days, use a vernier caliper to measure the width of the tumor. After 12 weeks, the mice were sacrificed through cervical dislocation, and tumor tissues were excised and weighed.

miRNA target genes. TargetScanHuman Release v.7.2 (http://www.targetscan.org/vert_72/) was used to predict the biological targets of miRNAs. The target genes and their miRNA binding sites were predicted using this online tool.

Statistical analyses. SPSS 22.0 software (IBM Corp.) was used in this study. Measured data are presented as mean ± standard deviation (unless otherwise shown). One-way analysis of variance (ANOVA) was used to analyze the differences among ≥3 groups, followed by Tukey's post hoc test. Group means were compared using an unpaired, two-sided Student's t-test. Wilcoxon signed-rank test was used to compare the expression of let-7f-1-3p in paracarcinoma and carcinoma tissues. P<0.05 was considered to indicate a statistically significant difference.

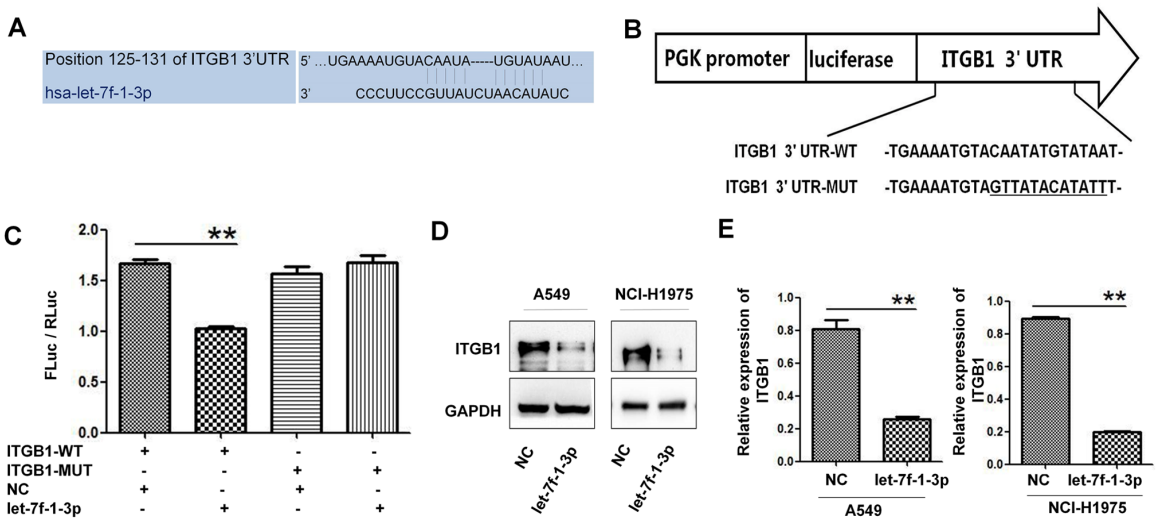

Figure 3. let-7f-1-3p directly targets ITGB1. (A) 3' UTR of the ITGB1 gene target sites of let-7f-1-3p were predicted using TargetScan. (B) Targeted binding sites and mutation sites of ITGB1 and let-7f-1-3p. (C) Luciferase assays in 293T cells transfected with WT or MUT 3' UTR report vector, NC or let-7f-1-3p. Whether let-7f-1-3p directly targeted ITGB1 in A549 and NCI-H1975 cells was determined via (D) western blotting and (E) densitometry analysis. **P<0.01. ITGB1, integrin β1; UTR, untranslated region; WT, wild-type; MUT, mutant; NC, negative control; PGK, phosphoglycerate kinase.

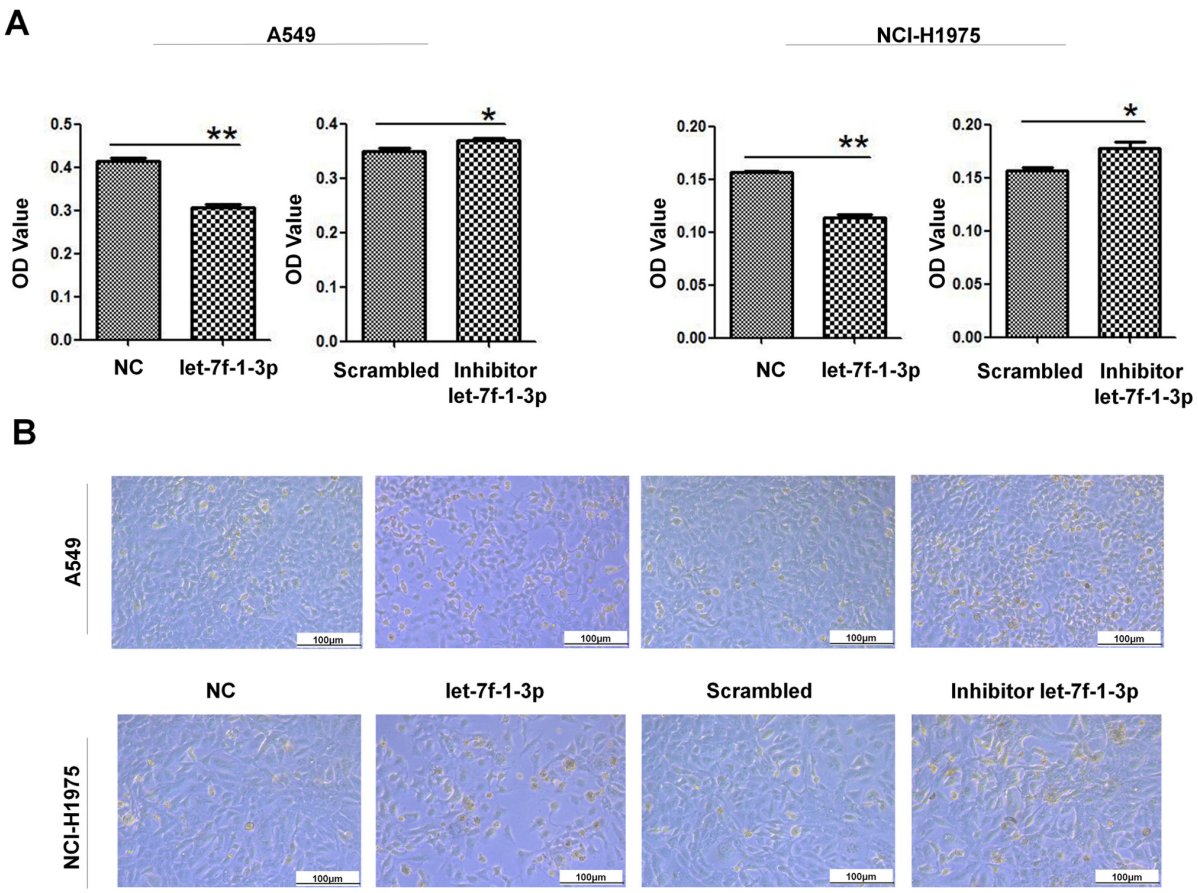

Figure 4. let-7f-1-3p inhibits the viability of NSCLC cells. Viability of A549 and NCI-H1975 cells transfected with let-7f-1-3p-mimics and let-7f-1-3p-inhibitor was detected using (A) MTT assays and (B) microscopy. *P<0.05, **P<0.01. NSCLC, non-small cell lung cancer; OD, optical density; NC, negative control.

Results

let-7f-1-3p is downregulated in NSCLC tissues. Although let-7f-1-3p is downregulated in human small airway epithelial cells (HSAEC) and human pulmonary alveolar epithelial cells (HPAEpiC) (26), let-7f-1-3p expression in NSCLC remains unclear. To identify the role of let-7f-1-3p in lung cancer, RT-qPCR was performed to detect the expression profile of let-7f-1-3p in NSCLC tissues. let-7f-1-3p expression levels were significantly decreased in NSCLC tissues compared with

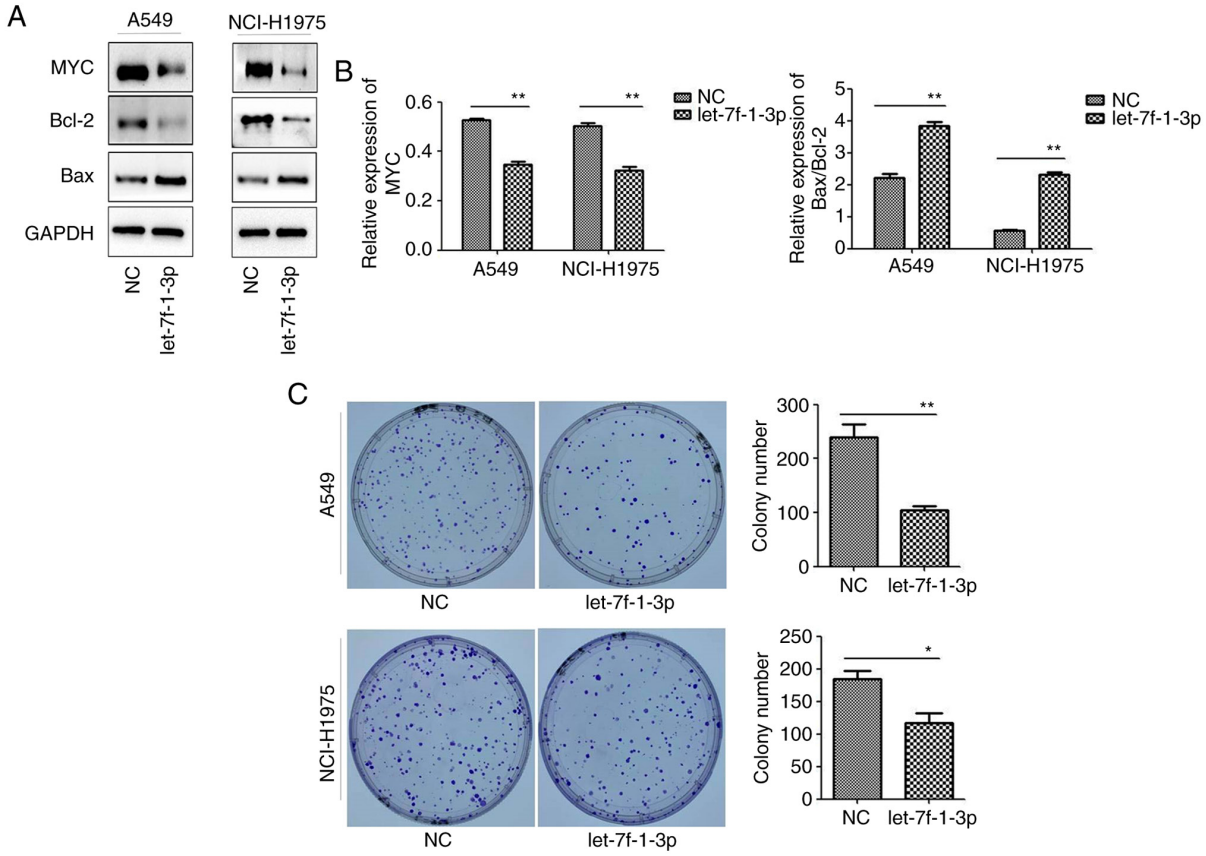

Figure 5. let-7f-1-3p affects apoptosis and decreases the number of colonies. (A) Western blot analysis and (B) densitometry analysis of the effects of let-7f-1-3p on Bax, MYC and Bcl-2 expression in A549 and NCI-H1975 cells. (C) Effects of let-7f-1-3p on the colony formation of A549 and NCI-H1975 cells. *P<0.05, **P<0.01. NC, negative control.

those in adjacent paracarcinoma tissues (Fig. 1A), suggesting the suppressive role of let-7f-1-3p in tumorigenesis of lung cancer. Thus, lower levels of let-7f-1-3p may be associated with NSCLC development.

Next, the expression levels of ITGB1 protein in patients with NSCLC were examined, which revealed that ITGB1 expression in NSCLC tissues was higher compared with in adjacent tissues (Fig. 1B). These results suggested that increased expression levels of ITGB1 may be associated with NSCLC development.

let-7f-1-3p expression decreases in NSCLC cell lines. To further investigate whether let-7f-1-3p inhibited the proliferation of NSCLC, let-7f-1-3p expression levels were detected in HBE, A549 and NCI-H1975 cells using RT-qPCR. let-7f-1-3p expression was significantly decreased in A549 and NCI-H1975 cells compared with HBE cells as a control group (Fig. 2A). Therefore, the A549 and NCI-H1975 cell lines were selected to be transfected with the let-7f-1-3p oligonucleotide. As presented in Fig. 2B, the expression levels of let-7f-1-3p in the two cell lines transfected with let-7f-1-3p mimics were upregulated compared with the cells transfected with NC. Conversely, let-7f-1-3p expression levels were significantly downregulated by transfection with the let-7f-1-3p inhibitor compared with the NC (Fig. 2C).

let-7f-1-3p directly regulates the expression of ITGB1. To gain insight into the molecular mechanism of let-7f-1-3p in suppressing lung cancer, ITGB1 was predicted to be a target gene of let-7f-1-3p using the TargetScan database (Fig. 3A). Subsequently, the ITGB1-3' UTR-WT vector and its mutant vector were constructed for transfection of let-7f-1-3p or NC into 293T cells (Fig. 3B). After 48 h, double-luciferase reporter gene assays indicated that the luciferase activity of the ITGB1-3' UTR-WT vector was significantly inhibited when the cells were co-transfected with let-7f-1-3p compared with the NC. However, there was no significant change in luciferase activity in cells co-transfected with ITGB1-3' UTR-MUT and let-7f-1-3p compared with those co-transfected with ITGB1-3' UTR-MUT and NC (Fig. 3C). Subsequently, western blotting suggested that the expression levels of ITGB1 were significantly downregulated in let-7f-1-3p-treated A549 and NCI-H1975 cells compared with the NC (Fig. 3D and E). In summary, these observations suggested that let-7f-1-3p targeted ITGB1 inhibition.

let-7f-1-3p inhibits the viability of NSCLC cells. To explore the effect of let-7f-1-3p on the viability of NSCLC cells, an MTT assay was used to detect the effect of cell viability after overexpression or inhibition of let-7f-1-3p. Cell viability was inhibited after let-7f-1-3p-overexpression compared with the NC in both A549 and NCI-H1975 cells, whereas the let-7f-1-3p-inhibitor significantly increased cell viability in the cells compared with that of the control group (Fig. 4A). Subsequently, the effect of the oligonucleotides on A549/NCI-H1975 cells was analyzed morphologically. After 48 h of treatment, overexpression of

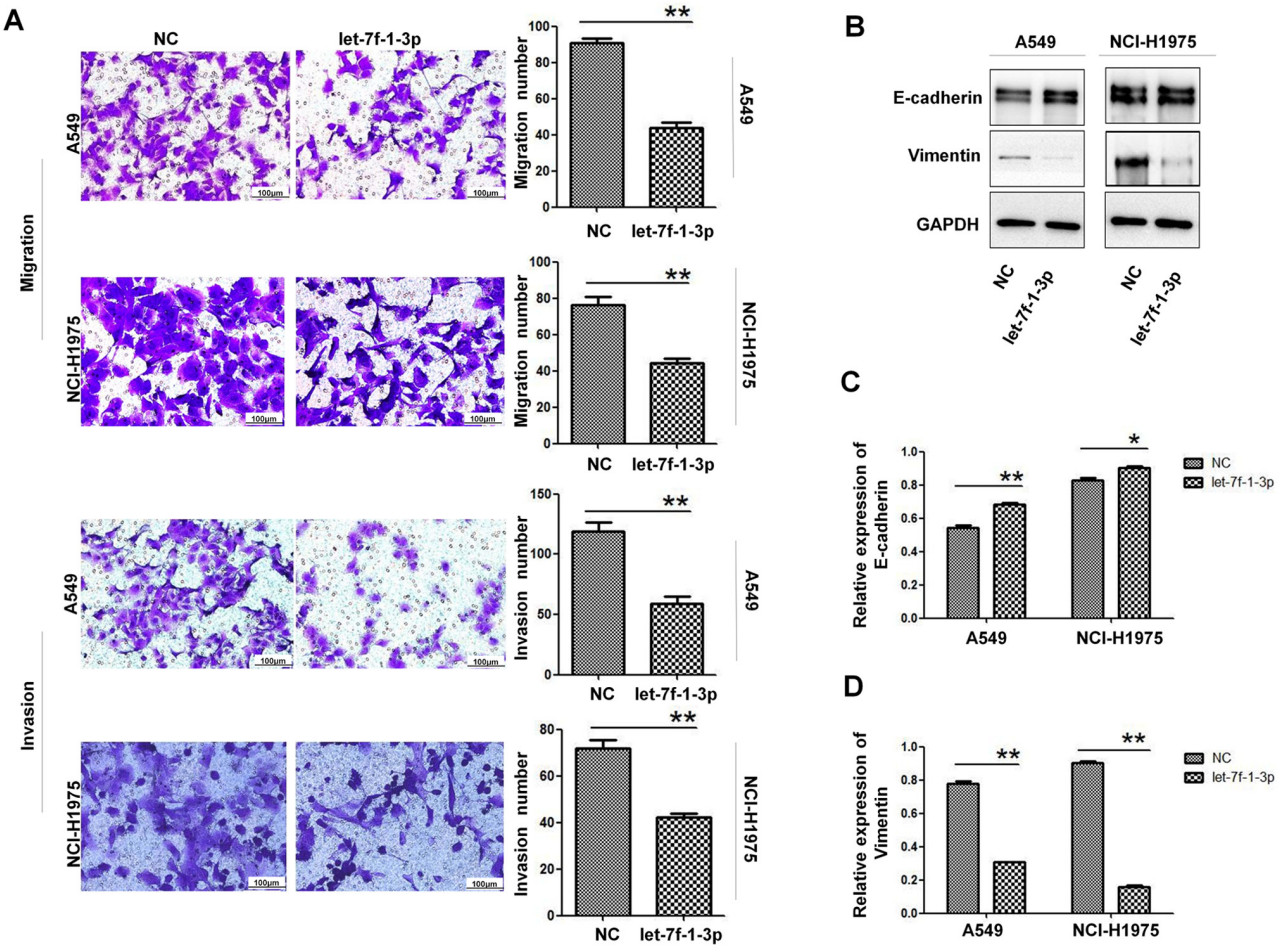

Figure 6. let-7f-1-3p inhibits cell migration and invasion. (A) Migration and invasion abilities of let-7f-1-3p-overexpressing A549 and NCI-H1975 cells and transfected NC cells were examined using Transwell assays. The number of migrating and invading cells treated with let-7f-1-3p decreased compared with the control. (B) Western blotting and densitometry analysis of (C) E-cadherin and (D) vimentin protein levels after let-7f-1-3p-overexpression in A549 and NCI-H1975 cells. *P<0.05, **P<0.01. NC, negative control.

let-7f-1-3p decreased the number of cells and their adhesion compared with the NC; by contrast, inhibition of let-7f-1-3p increased the number of cells (Fig. 4B).

let-7f-1-3p affects apoptosis and decreases the colony number of NSCLC cells. To explore the molecular mechanism of the let-7f-1-3p-induced effects on NSCLC cells, the expression levels of apoptosis-related proteins were analyzed. After let-7f-1-3p was overexpressed for 48 h, the Bax/Bcl-2 ratio significantly increased, whereas the expression of MYC significantly decreased, as determined via western blotting (Fig. 5A and B). Cell clone formation experiments supported these results, as let-7f-1-3p overexpression significantly decreased the colony numbers compared with the NC (Fig. 5C).

let-7f-1-3p inhibits cell migration and invasion. Given that the malignancy of tumor cells is closely associated with their local infiltration and distant migratory ability, the effect of let-7f-1-3p on the migration and invasion of NSCLC cells was investigated. The results revealed that the migratory ability of A549 and NCI-H1975 cells overexpressing let-7f-1-3p was significantly decreased compared with the NC group (Fig. 6A). Moreover, let-7f-1-3p-overexpression inhibited the invasive ability of A549 and NCI-H1975 cells compared with the NC cells (Fig. 6A). Furthermore, let-7f-1-3p-overexpression increased the expression levels of E-cadherin (an epithelial cell marker) and reduced the expression levels of vimentin (a mesenchymal cell marker; Fig. 6B-D). These results suggested that let-7f-1-3p suppressed the migration and invasion ability of NSCLC.

Suppressive role of let-7f-1-3p is attenuated by the overexpression of ITGB1. Given that let-7f-1-3p suppressed the migration and invasion of A549 and NCI-H1975 cells, whether overexpression of ITGB1 could attenuate the effects of let-7f-1-3p was investigated. First, the transfection efficiency was detected via RT-qPCR. As presented in Fig. 7A, the expression level of ITGB1 in two cell lines after overexpression was significantly increased compared with the control. A549 and NCI-H1975 cells were treated with NC + pcDNA3.1-3*Flag, NC + pcDNA3.1-ITGB1-3*Flag, let-7f-1-3p mimics + pcDNA3.1-3*Flag and let-7f-1-3p mimics + pcDNA3.1-ITGB1-3*Flag. The results of the MTT assays suggested that the viability potential of A549 and NCI-H1975 cells transfected with let-7f-1-3p and ITGB1 was significantly increased compared with that of let-7f-1-3p and pcDNA3.1-3*Flag (Fig. 7B). Moreover, the Transwell assay results demonstrated that the migration and invasion ability

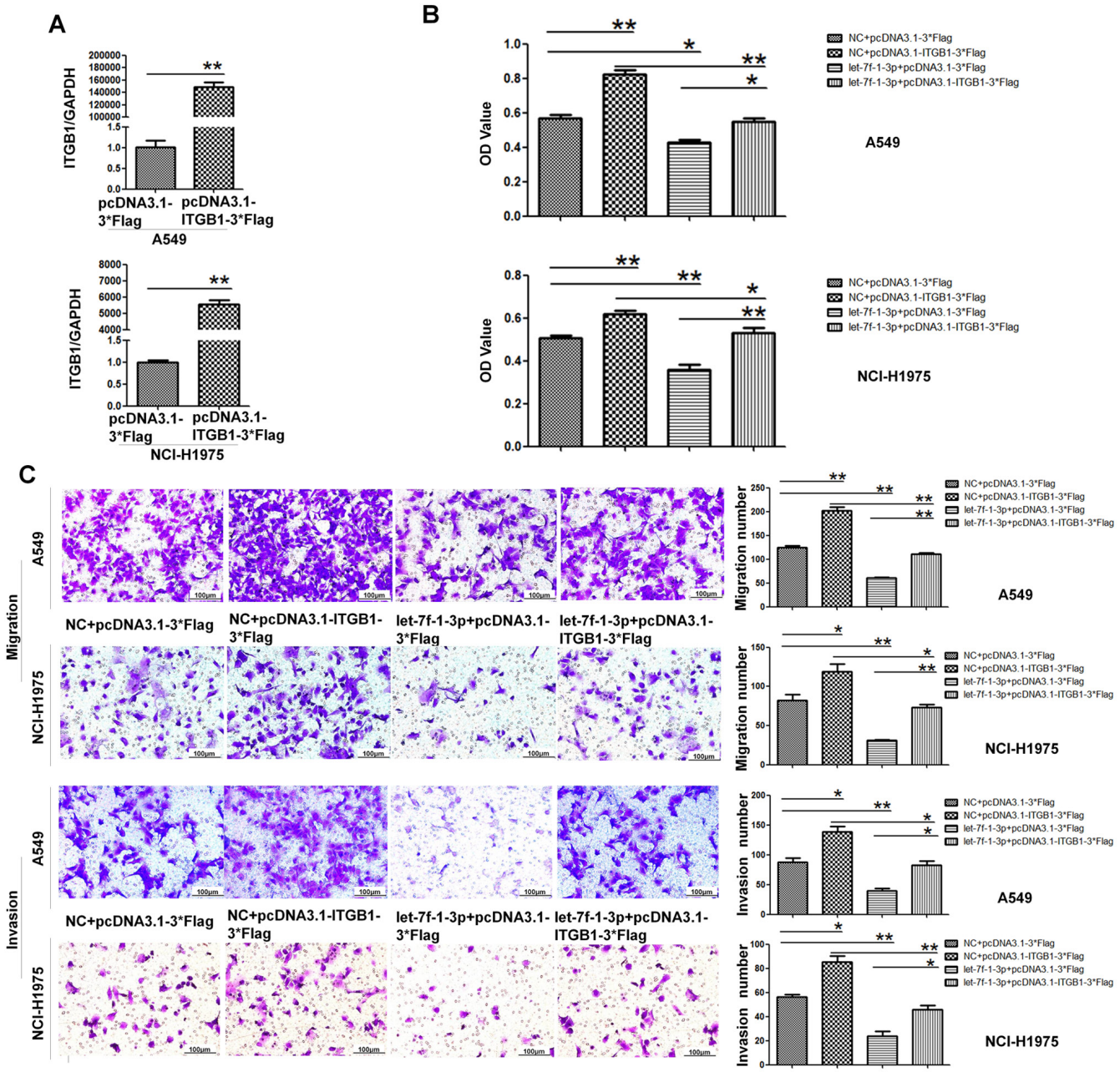

Figure 7. ITGB1 reverses the suppressive effects of let-7f-1-3p on NSCLC cells. (A) Reverse transcription-quantitative PCR analysis of exogenous ITGB1 expression after transfection of pcDNA3.1-3*Flag (empty vector) and pcDNA3.1-ITGB1-3*Flag in A549 and NCI-H1975 cells. (B) Viability of A549 and NCI-H1975 cells transfected with NC + pcDNA3.1-3*Flag, NC + pcDNA3.1-ITGB1-3*Flag, let-7f-1-3p mimics + pcDNA3.1-3*Flag and let-7f-1-3p mimics + pcDNA3.1-ITGB1-3*Flag were detected using MTT assays. (C) Migration and invasion abilities of let-7f-1-3p and ITGB1-overexpressing A549 and NCI-H1975 cells and transfected control cells were examined via Transwell assays and quantified. *P<0.05, **P<0.01. ITGB1, integrin β1; OD, optical density; NC, negative control.

of the let-7f-1-3p + ITGB1 overexpression group was significantly increased compared with the let-7f-1-3p mimics + pcDNA3.1-3*Flag group (Fig. 7C). In conclusion, these data revealed that let-7f-1-3p inhibited cell viability, migration and invasion by targeting ITGB1.

let-7f-1-3p promotes the role of DOX in apoptosis and in inhibiting cell viability, migration and invasion in vitro. To evaluate the biological consequences of DOX on the development of NSCLC cells, viability assays and western blotting were performed. The MTT assay revealed that the viability of A549 cells treated with 0, 200, 400, 600, and 800 ng/ml DOX gradually but significantly decreased (Fig. 8A). In addition, DOX treatment markedly inhibited A549 cell proliferation (Fig. 8B). Next, DOX was revealed to significantly inhibit ITGB1 expression in A549 cells (Fig. 8C).

Given that DOX suppressed the proliferation of A549 cells, whether combining DOX with let-7f-1-3p hindered cell proliferation was investigated. A549 cells were treated with NC + DOX (200 ng/ml) and let-7f-1-3p mimics + DOX (200 ng/ml). The number of surviving A549 cells after treatment with let-7f-1-3p mimics and DOX was decreased compared with that in the control group and the let-7f-1-3p group (Fig. 8D). Moreover, a significantly decreased number of clones was observed in the co-treated let-7f-1-3p mimics and DOX group compared with the let-7f-1-3p mimics group (Fig. 8E).

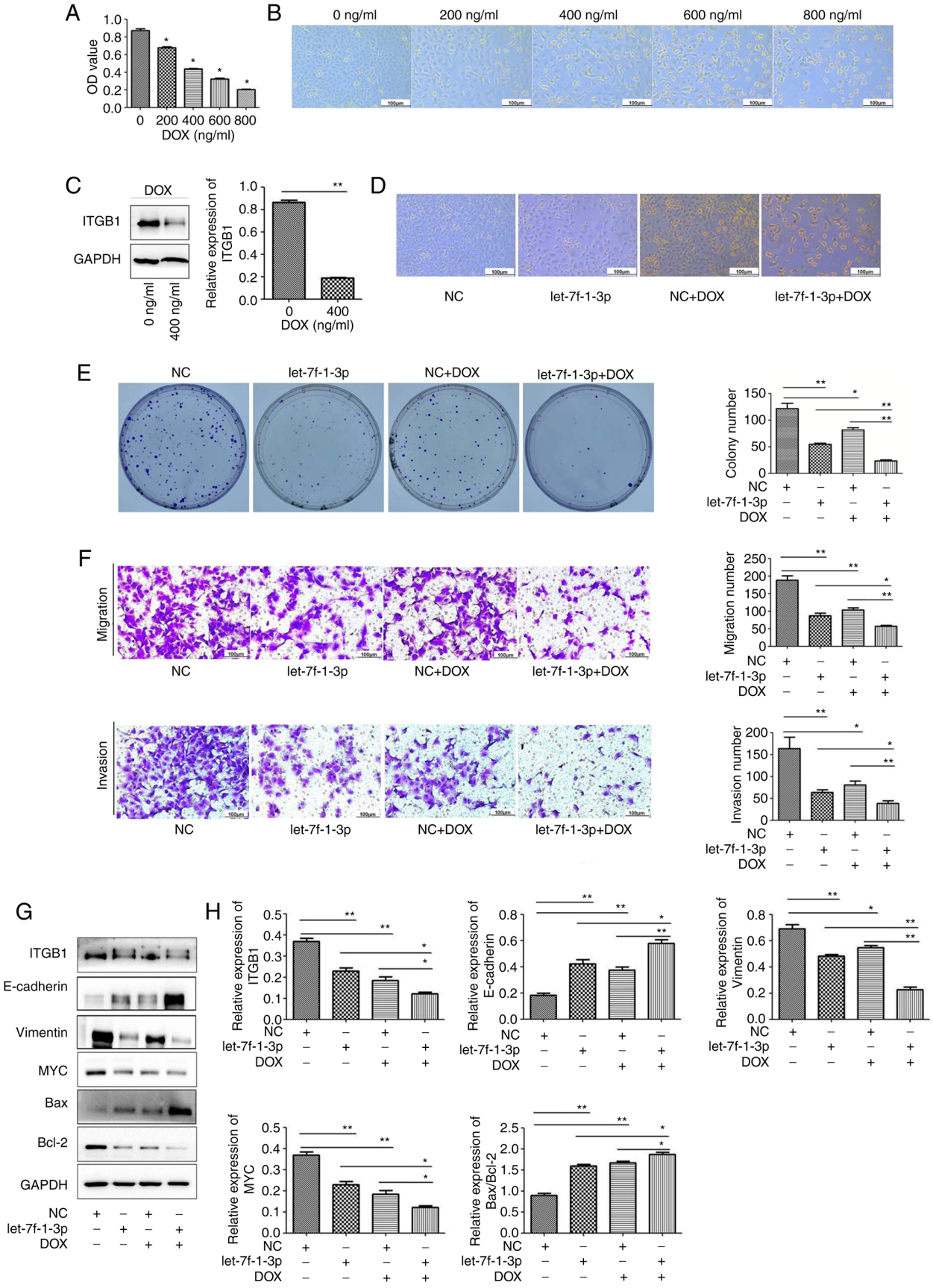

Figure 8. let-7f-1-3p promotes the roles of DOX in cell apoptosis, viability, migration, and invasion *in vitro*. (A) DOX significantly inhibited A549 cell viability in a dose-dependent manner in the MTT assay. *P<0.05 vs. 0 ng/ml. (B) Fewer living A549 cells were identified in the DOX-treated lung adenocarcinoma cultures compared with the control cells (scale bar, 100 μm). (C) DOX (400 ng/ml) suppressed ITGB1 expression in A549 cells, as shown via western blotting on the left and densitometry analysis on the right. (D) Changes in the number of cells were detected via microscopy after NC, let-7f-1-3p mimics, NC + DOX and let-7f-1-3p mimics + DOX treatment. (E) Colonies from the cell treatment groups are indicated on the left, and colony formation ability is shown on the right (scale bar, 100 μm). (F) Images of cell migration and invasion are shown on the left and quantified on the right. (G) Western blotting and (H) densitometry analysis results of ITGB1, E-cadherin, vimentin, MYC, Bax and Bcl-2. *P<0.05, **P<0.01. DOX, doxorubicin; NC, negative control; OD, optical density; ITGB1, integrin β1.

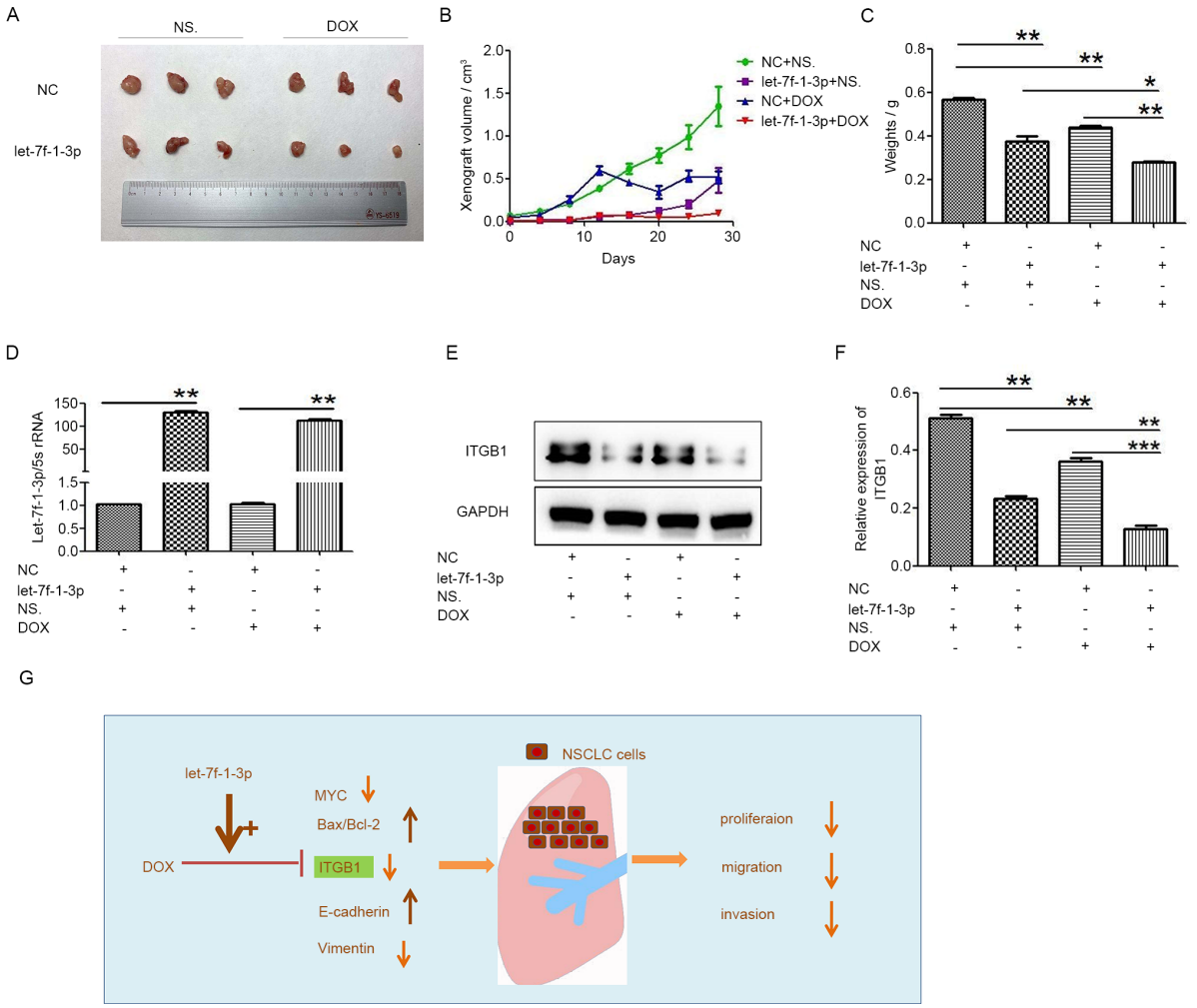

Figure 9. DOX and let-7f-1-3p suppress cancer progression *in vivo*. (A) Volumes of A549 cancer xenografts were detected after NC + saline, let-7f-1-3p mimics + saline, NC + DOX, and let-7f-1-3p mimics + DOX treatments. (B) Tumor volumes and (C) weights were the smallest when treated with let-7f-1-3p mimics + DOX treatment. (D) Expression of let-7f-1-3p in nude mouse tumors was analyzed using reverse transcription-quantitative PCR. (E) Western blotting and (F) quantification of ITGB1 expression in tumors treated with let-7f-1-3p mimics + DOX compared with control tumors (G) Compared with let-7f-1-3p group, Bax/Bcl-2 ratio and E-cadherin were significantly increased, while the expression of MYC and vimentin were significantly decreased, indicating that let-7f-1-3p overexpression and DOX inhibited NSCLC cell proliferation and migration. *P<0.05, **P<0.01, ***P<0.001. DOX, doxorubicin; NC, negative control; ITGB1, integrin β1; rRNA, ribosomal RNA; NSCLC, non-small cell lung cancer; NS, Normal saline.

Consistent with the aforementioned experiments, the results demonstrated that the number of let-7f-1-3p-overexpressing + DOX clones that passed through the Transwell chambers were significantly decreased compared with the number of let-7f-1-3p group that passed through the chambers (Fig. 8F). The treatment with let-7f-1-3p + DOX significantly suppressed the expression of ITGB1, vimentin and Bcl-2 compared with single miRNA or DOX treatment (Fig. 8G and H). These data suggested that the promotive effect of let-7f-1-3p on the anticancer roles of DOX was associated with the regulation of ITGB1.

let-7f-1-3p and DOX suppress cancer progression in vivo. To further address the tumor-suppressive role of let-7f-1-3p in promoting the effect of DOX on NSCLC, A549 cells transfected with NC and let-7f-1-3p mimics were injected into BALB/c nude mice to establish A549 lung cancer xenografts, then the mice with xenografts were treated with DOX. When let-7f-1-3p was overexpressed, the xenograft growth measured in tumor size, volume and weight was decreased compared with that of the corresponding control group (Fig. 9A-C). Moreover, the tumor growth curves indicated that the tumor volume in let-7f-1-3p + DOX mice decreased compared with that in let-7f-1-3p or DOX-treated mice (Fig. 9A and B). Compared with the NC+NS group, let-7f-1-3p in the let-7f-1-3p+NS group was significantly increased. Compared with the NC+DOX group, let-7f-1-3p was significantly upregulated in the let-7f-1-3p+DOX group (Fig. 9D). ITGB1 expression significantly decreased in both let-7f-1-3p and DOX-treated mice compared with that in let-7f-1-3p or DOX-treated xenografts (Fig. 9E and F). In summary, these results demonstrated that let-7f-1-3p and DOX co-treatment significantly suppressed cancer progression via ITGB1 *in vivo*.

Discussion

As a small non-coding RNA, miRNA can promote or inhibit tumor development and play a regulatory role in cancer metastasis. For example, miR-200 inhibits epithelial-to-mesenchymal transition and tumorigenic effects by targeting quaking (27).

In triple-negative breast cancer, miR-200c promotes apoptosis by directly targeting phosphodiesterase 7B (28). miR-532-3p is negatively associated with the kinesin family member C11 expression, leading to metastasis via the activation of the gankyrin/AKT signaling pathway in hepatocellular carcinoma (29). Han *et al* (26) demonstrated that let-7f attenuates smoke-induced apoptosis in HSAEC and HPAEpiC. In the present study, let-7f-1-3p suppressed the proliferation of NSCLC cells *in vitro* and *in vivo* by directly decreasing ITGB1 expression. Furthermore, let-7f-1-3p overexpression reduced MYC expression and upregulated the Bax/Bcl-2 ratio. let-7f-1-3p also inhibited the migration and invasion of NSCLC by increasing the expression of E-cadherin and decreasing the expression of vimentin. Moreover, let-7f-1-3p promoted the ability of DOX to inhibit cell viability, migration and invasion both *in vitro* and *in vitro* (Fig. 9G).

Integrins directly bind to the components of the extracellular matrix and provide the traction necessary for cell motility and invasion (30). ITGB1, a potential oncoprotein, contributes to tumor growth and migration (31). In the present study, let-7f-1-3p was negatively associated with ITGB1, which was consistent with the results of DOX treatment. Moreover, the expression levels of ITGB1 increased in NSCLC tissues compared with paracancerous lung tissues. ITGB1 plays a notable role in mediating metastatic dissemination and preventing tumor cell senescence (32). In addition to migration and invasion, integrins can regulate proliferation (33). In particular, let-7f-1-3p prevents tumor viability, migration and invasion by regulating ITGB1.

The co-treatment of DOX and miRNA has been used in the treatment process of multiple animal cancer models (34,35). miR-101/DOX-liposome suppresses the malignant progression of liver cancer cells *in vitro* and *in vivo* through the combinatory effect on miR-101 and DOX (34). Zhang *et al* (36) revealed that combining DOX and miR-21 inhibitor significantly increases the expression of tumor suppressor genes to reduce tumor cell proliferation, invasion and migration in glioblastoma cells compared with the effect of DOX or miR-21 inhibitor treatment alone. Moreover, co-delivering miR-159 and DOX contributed to the treatment of triple-negative breast cancer (35). The viability of breast cancer cells treated with DOX and miR-154 mimic considerably decreased compared with that of cells treated with DOX alone (37). Furthermore, miR-608 enhances the efficacy of DOX in the treatment of NSCLC by suppressing the expression of transcription factor-activated enhancer-binding protein 4 (38). The present study demonstrated that let-7f-1-3p and DOX suppressed not only cancer progression by ITGB1 but also viability, migration and invasion.

The present study did not further explore the ways in which DOX's inhibitory effect on ITGB1 inhibits the development of NSCLC. It can be speculated that DOX may affect the expression of ITGB1 by regulating the expression of an intermediate molecule. Follow-up studies should use co-immunoprecipitation to identify molecules that interact with ITGB1, to construct the molecular regulatory network of ITGB1 and provide new clinical treatment strategies for NSCLC.

In summary, the current study provided novel evidence that let-7f-1-3p acted as a tumor suppressor in inhibiting the viability of NSCLC by targeting ITGB1. let-7f-1-3p can also promote the anticancer ability of DOX by inhibiting the development of NSCLC. Future studies will continue to investigate the specific mechanism by which DOX regulates the development of NSCLC.

Acknowledgements

Not applicable.

Funding

The present study was supported by National Natural Science Foundation of China (grant nos. 81800169, 81772281 and 81702296), Shandong Science and Technology Committee (grant nos. 2018GSF118056 and ZR2019MH022), Foundation of Shandong Educational Committee (grant nos. J17KA121 and 2019KJK014), Yantai Science and Technology Committee (grant no. 2018XSCC051) and Shandong Province Taishan Scholar Project (grant no. ts201712067).

Availability of data and materials

All data generated or analyzed during this study are included in this published article.

Authors' contributions

YaY, YuL, NX, YS, LS, HS, YW and YuY performed the experiment. YaY, YuL and YoL drafted the manuscript. YuY, PW and YS analyzed the data. YS, YoL and SX contributed in experimental design and manuscript revision. SX, YuL and YaY conceived the study, designed the experiment, and finalized the manuscript. YaY and YuL confirmed the authenticity of all the raw data. All authors read and approved the final manuscript.

Ethics approval and consent to participate

All experiments with human specimens were performed in accordance with the relevant guidelines and were approved by The Medical Ethics Committee of Binzhou Medical University (Yantai, China; approval number: 2018-07-06). Prior to study inclusion, written informed consent was obtained from all patients. All animal experiments in the present study were approved by The Committee on the Ethics of Animal Experiments of Binzhou Medical University (approval number: 2018-07-06).

Patient consent for publication

Not applicable.

Competing interests

The authors declare that they have no competing interests.

References

1. Bray F, Ferlay J, Soerjomataram I, Siegel RL, Torre LA and Jemal A: Global cancer statistics 2018: GLOBOCAN estimates of incidence and mortality worldwide for 36 cancers in 185 countries. CA Cancer J Clin 68: 394-424, 2018.

2. Feng H, Ge F, Du L, Zhang Z and Liu D: MiR-34b-3p represses cell proliferation, cell cycle progression and cell apoptosis in non-small-cell lung cancer (NSCLC) by targeting CDK4. J Cell Mol Med 23: 5282-5291, 2019.
3. Lang N, Wang C, Zhao J, Shi F, Wu T and Cao H: Long noncoding RNA BCYRN1 promotes glycolysis and tumor progression by regulating the miR149/PKM2 axis in nonsmallcell lung cancer. Mol Med Rep 21: 1509-1516, 2020.
4. Zou A, Liu X, Mai Z, Zhang J, Liu Z, Huang Q, Wu A and Zhou C: LINC00472 acts as a tumor suppressor in NSCLC through KLLN-mediated p53-signaling pathway via MicroRNA-149-3p and MicroRNA-4270. Mol Ther Nucleic Acids 17: 563-577, 2019.
5. Dai FQ, Li CR, Fan XQ, Tan L, Wang RT and Jin H: miR-150-5p inhibits non-small-cell lung cancer metastasis and recurrence by targeting HMGA2 and β-catenin signaling. Mol Ther Nucleic Acids 16: 675-685, 2019.
6. Wang W, Shen XB, Jia W, Huang DB, Wang Y and Pan YY: The p53/miR-193a/EGFR feedback loop function as a driving force for non-small cell lung carcinoma tumorigenesis. Ther Adv Med Oncol 11: 1758835919850665, 2019.
7. Liu X, Min S, Wu N, Liu H, Wang T, Li W, Shen Y, Zhao C, Wang H, Qian Z, *et al*: miR-193a-3p inhibition of the Slug activator PAK4 suppresses non-small cell lung cancer aggressiveness via the p53/Slug/L1CAM pathway. Cancer Lett 447: 56-65, 2019.
8. Che Y, Shi X, Shi Y, Jiang X, Ai Q, Shi Y, Gong F and Jiang W: Exosomes derived from miR-143-overexpressing MSCs inhibit cell migration and invasion in human prostate cancer by down-regulating TFF3. Mol Ther Nucleic Acids 18: 232-244, 2019.
9. Gu C, Cai J, Xu Z, Zhou S, Ye L, Yan Q, Zhang Y, Fang Y, Liu Y, Tu C, *et al*: MiR-532-3p suppresses colorectal cancer progression by disrupting the ETS1/TGM2 axis-mediated Wnt/beta-catenin signaling. Cell Death Dis 10: 739, 2019.
10. Tung CH, Kuo LW, Huang MF, Wu YY, Tsai YT, Wu JE, Hsu KF, Chen YL and Hong TM: MicroRNA-150-5p promotes cell motility by inhibiting c-Myb-mediated Slug suppression and is a prognostic biomarker for recurrent ovarian cancer. Oncogene 39: 862-876, 2020.
11. Shen GY, Ren H, Shang Q, Zhao WH, Zhang ZD, Yu X, Huang JJ, Tang JJ, Yang ZD, Liang D and Jiang XB: Let-7f-5p regulates TGFBR1 in glucocorticoid-inhibited osteoblast differentiation and ameliorates glucocorticoid-induced bone loss. Int J Biol Sci 15: 2182-2197, 2019.
12. Tan W, Gu Z, Leng J, Zou X, Chen H, Min F, Zhou W, Zhang L and Li G: Let-7f-5p ameliorates inflammation by targeting NLRP3 in bone marrow-derived mesenchymal stem cells in patients with systemic lupus erythematosus. Biomed Pharmacother 118: 109313, 2019.
13. Li ZH, Wang YF, He DD, Zhang XM, Zhou YL, Yue H, Huang S, Fu Z, Zhang LY, Mao ZQ, *et al*: Let-7f-5p suppresses Th17 differentiation via targeting STAT3 in multiple sclerosis. Aging (Albany NY) 11: 4463-4477, 2019.
14. Gao XR, Ge J, Li WY, Zhou WC, Xu L and Geng DQ: NF-kappaB/let-7f-5p/IL-10 pathway involves in wear particle-induced osteolysis by inducing M1 macrophage polarization. Cell Cycle 17: 2134-2145, 2018.
15. Shen GY, Ren H, Huang JJ, Zhang ZD, Zhao WH, Yu X, Shang Q, Qiu T, Zhang YZ, Tang JJ, *et al*: Plastrum testudinis extracts promote BMSC proliferation and osteogenic differentiation by regulating Let-7f-5p and the TNFR2/PI3K/AKT signaling pathway. Cell Physiol Biochem 47: 2307-2318, 2018.
16. Han L, Zhou Y, Zhang R, Wu K, Lu Y, Li Y, Duan R, Yao Y, Zhu D and Jia Y: MicroRNA Let-7f-5p promotes bone marrow mesenchymal stem cells survival by targeting caspase-3 in Alzheimer disease model. Front Neurosci 12: 333, 2018.
17. Tie Y, Chen C, Yang Y, Qian Z, Yuan H, Wang H, Tang H, Peng Y, Du X and Liu B: Upregulation of let-7f-5p promotes chemotherapeutic resistance in colorectal cancer by directly repressing several pro-apoptotic proteins. Oncol Lett 15: 8695-8702, 2018.
18. Di Fazio P, Maass M, Roth S, Meyer C, Grups J, Rexin P, Bartsch DK and Kirschbaum A: Expression of hsa-let-7b-5p, hsa-let-7f-5p, and hsa-miR-222-3p and their putative targets HMGA2 and CDKN1B in typical and atypical carcinoid tumors of the lung. Tumour Biol 39: 1010428317728417, 2017.
19. Chang J, Huang L, Cao Q and Liu F: Identification of colorectal cancer-restricted microRNAs and their target genes based on high-throughput sequencing data. Onco Targets Ther 9: 1787-1794, 2016.
20. Cui J, Huang W, Wu B, Jin J, Jing L, Shi WP, Liu ZY, Yuan L, Luo D, Li L, *et al*: N-glycosylation by N-acetylglucosaminyltransferase V enhances the interaction of CD147/basigin with integrin beta1 and promotes HCC metastasis. J Pathol 245: 41-52, 2018.
21. Zhao G, Gong L, Su D, Jin Y, Guo C, Yue M, Yao S, Qin Z, Ye Y, Tang Y, *et al*: Cullin5 deficiency promotes small-cell lung cancer metastasis by stabilizing integrin β1. J Clin Invest 129: 972-987, 2019.
22. Wang X, Zhou Q, Yu Z, Wu X, Chen X, Li J, Li C, Yan M, Zhu Z, Liu B and Su L: Cancer-associated fibroblast-derived Lumican promotes gastric cancer progression via the integrin beta1-FAK signaling pathway. Int J Cancer 141: 998-1010, 2017.
23. Izumi D, Ishimoto T, Miyake K, Sugihara H, Eto K, Sawayama H, Yasuda T, Kiyozumi Y, Kaida T, Kurashige J, *et al*: CXCL12/CXCR4 activation by cancer-associated fibroblasts promotes integrin beta1 clustering and invasiveness in gastric cancer. Int J Cancer 138: 1207-1219, 2016.
24. Wu JI, Lin YP, Tseng CW, Chen HJ and Wang LH: Crabp2 promotes metastasis of lung cancer cells via HuR and integrin β1/FAK/ERK signaling. Sci Rep 9: 845, 2019.
25. Hou J, Lin L, Zhou W, Wang Z, Ding G, Dong Q, Qin L, Wu X, Zheng Y, Yang Y, *et al*: Identification of miRNomes in human liver and hepatocellular carcinoma reveals miR-199a/b-3p as therapeutic target for hepatocellular carcinoma. Cancer Cell 19: 232-243, 2011.
26. Han Z, Zhu Y, Cui Z, Guo P, Wei A and Meng Q: MicroRNA Let-7f-1-3p attenuates smoke-induced apoptosis in bronchial and alveolar epithelial cells in vitro by targeting FOXO1. Eur J Pharmacol 862: 172531, 2019.
27. Kim EJ, Kim JS, Lee S, Lee H, Yoon JS, Hong JH, Chun SH, Sun S, Won HS, Hong SA, *et al*: QKI, a miR-200 target gene, suppresses epithelial-to-mesenchymal transition and tumor growth. Int J Cancer 145: 1585-1595, 2019.
28. Zhang DD, Li Y, Xu Y, Kim J and Huang S: Phosphodiesterase 7B/microRNA-200c relationship regulates triple-negative breast cancer cell growth. Oncogene 38: 1106-1120, 2019.
29. Han J, Wang F, Lan Y, Wang J, Nie C, Liang Y, Song R, Zheng T, Pan S, Pei T, *et al*: KIFC1 regulated by miR-532-3p promotes epithelial-to-mesenchymal transition and metastasis of hepatocellular carcinoma via gankyrin/AKT signaling. Oncogene 38: 406-420, 2019.
30. Desgrosellier JS and Cheresh DA: Integrins in cancer: Biological implications and therapeutic opportunities. Nat Rev Cancer 10: 9-22, 2010.
31. Chen MB, Lamar JM, Li R, Hynes RO and Kamm RD: Elucidation of the roles of tumor integrin β1 in the extravasation stage of the metastasis cascade. Cancer Res 76: 2513-2524, 2016.
32. Kren A, Baeriswyl V, Lehembre F, Wunderlin C, Strittmatter K, Antoniadis H, Fässler R, Cavallaro U and Christofori G: Increased tumor cell dissemination and cellular senescence in the absence of beta1-integrin function. EMBO J 26: 2832-2842, 2007.
33. Assoian RK and Klein EA: Growth control by intracellular tension and extracellular stiffness. Trends Cell Biol 18: 347-352, 2008.
34. Xu F, Liao JZ, Xiang GY, Zhao PX, Ye F, Zhao Q and He XX: MiR-101 and doxorubicin codelivered by liposomes suppressing malignant properties of hepatocellular carcinoma. Cancer Med 6: 651-661, 2017.
35. Gong C, Tian J, Wang Z, Gao Y, Wu X, Ding X, Qiang L, Li G, Han Z, Yuan Y and Gao S: Functional exosome-mediated co-delivery of doxorubicin and hydrophobically modified microRNA 159 for triple-negative breast cancer therapy. J Nanobiotechnology 17: 93, 2019.
36. Zhang S, Han L, Wei J, Shi Z, Pu P, Zhang J, Yuan X and Kang C: Combination treatment with doxorubicin and microRNA-21 inhibitor synergistically augments anticancer activity through upregulation of tumor suppressing genes. Int J Oncol 46: 1589-1600, 2015.
37. Bolandghamat Pour Z, Nourbakhsh M, Mousavizadeh K, Madjd Z, Ghorbanhosseini SS, Abdolvahabi Z, Hesari Z and Ezzati Mobasser S: Suppression of nicotinamide phosphoribosyltransferase expression by miR-154 reduces the viability of breast cancer cells and increases their susceptibility to doxorubicin. BMC Cancer 19: 1027, 2019.
38. Wang YF, Ao X, Liu Y, Ding D, Jiao WJ, Yu Z, Zhai WX, Dong SH, He YQ, Guo H and Wang JX: MicroRNA-608 promotes apoptosis in non-small cell lung cancer cells treated with doxorubicin through the inhibition of TFAP4. Front Genet 10: 809, 2019.